Liquefaction Assessment and Soil Spatial Variation

José León González Acosta(✉), Abraham P. van den Eijnden, and Michael A. Hicks

Section of Geo-Engineering, Faculty of Civil Engineering and Geosciences, Delft University of Technology, Delft, The Netherlands
J.L.GonzalezAcosta-1@tudelft.nl

Abstract. Soil liquefaction is investigated considering a saturated soil deposit and by implementing standard techniques of random field theory to distribute initial void ratio values and assess liquefaction risk. The soil domain is represented in a 2-dimensional (2D) random finite element model for the dynamic analysis of coupled behavior. Multiple Monte Carlo realizations are subjected to a base acceleration, while cyclic and small strain soil behaviours are achieved through a hypoplastic constitutive model. This investigation demonstrates that 2D stochastic simulations converge to 2D deterministic simulations when small standard deviations and/or small scales of fluctuation are used. However, large standard deviations combined with relatively large scales of fluctuation may cause significant uncertainty in the response of the soil deposit. Finally, common techniques employed to assess soil liquefaction are evaluated based on the results of the deterministic and random field analyses.

Keywords: Coupled behaviour · Earthquakes · Hypoplasticity · Liquefaction · Random fields

1 Introduction

Soil liquefaction is a phenomenon for which the consequences can be catastrophic. The analysis and prediction of this phenomenon is typically achieved through 1D simulations in which a soil column, with a specific stratigraphy, is subjected to a base acceleration. The repeated loads of an earthquake can cause the compaction of loose soils, as well as the generation and accumulation of excess pore pressures, and may finally lead to the complete loss of the soil strength and the collapse of its structure (e.g. settlements). The main inconvenience of standard techniques used to investigate soil liquefaction is that a realistic distribution of soil properties is difficult to consider. The use of 1D columns neglects the effects of the soil attributes in the horizontal direction by which, in the presence of loose material pockets, liquefaction triggering can occur. To include the effects of a realistic distribution of soil properties in the domain, several authors have employed techniques based on random field theory (Fenton and VanMarcke 1998; Popescu et al. 2005). However, those studies were focused mainly on the analysis of specific case histories, and a comprehensive study of the consequences of parameter

M. Barla et al. (Eds.): IACMAG 2022, LNCE 288, pp. 283–290, 2023.
https://doi.org/10.1007/978-3-031-12851-6_34

variations, in particular with respect to (i) standard deviation and (ii) scales of fluctuation, remains to be done. This paper first introduces the concept of random field theory. Then, a benchmark is introduced to study soil liquefaction in a stochastic context, considering different standard deviations and scales of fluctuation. Liquefaction is assessed through surface accelerations and two liquefaction indexes.

2 Random Fields Theoretical Background

Random field methods are used to distribute parameters spatially over a domain. Fields of material properties are constructed through (i) a probability density function (pdf), described by a mean μ and standard deviation σ, in which $V = \sigma/\mu$ is the coefficient of variation, and (ii) a spatial correlation function, described by horizontal and vertical scales of fluctuation, θ_H and θ_V, respectively, representing the distances over which property values are significantly correlated. Figure 1a shows a sketch of a void ratio, *e*, distribution with depth and Fig. 1b shows the probability density function of *e*.

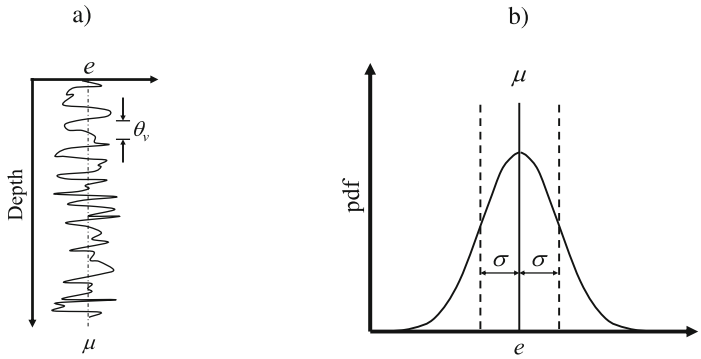

Fig. 1. a) Variation of void ratio *e* with depth, and b) probability density function of *e* (after Hicks and Samy 2002)

A comprehensive study of a boundary value problem using stochastic methods may be performed through Monte Carlo techniques, in which multiple realizations (i.e. simulations) are evaluated to derive a distribution of possible model outcomes. Note that each realization is performed considering a new set of randomly distributed properties (based on the same input statistics).

3 Initial Conditions and Liquefaction Assessment

In this paper, to ensure a comprehensive assessment of liquefaction triggering using random fields, a solution is first computed using a 2D domain of homogeneous material. This 2D solution will be used as the deterministic (D) solution. Then, a collection of Monte Carlo analyses will be performed, in which each group of simulations considers a constant mean void ratio e_μ, a void ratio standard deviation e_σ, and horizontal and

vertical scales of fluctuation, θ_H and θ_V, respectively. Note that constant values of e_μ, e_σ, θ_H and θ_V still result in different spatial distributions of void ratio within the domain for each realization. Figure 2 shows the acceleration record used to simulate the earthquake. The record corresponds to the North-South component of the Superstition Hills event. However, the simulated time was truncated at 12 s since the following data proved to be inconsequential.

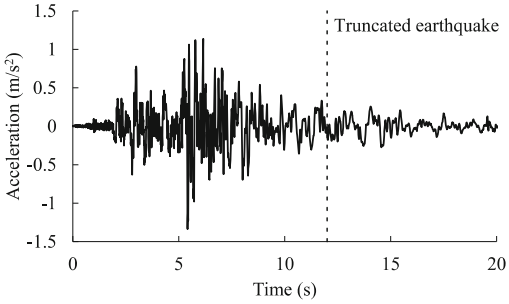

Fig. 2. Recorded accelerogram during Superstition Hills event (North-South component)

Regarding the domain's lateral boundary conditions, periodic boundaries (PB) were implemented (Cook et al. 1989). To test the code, a benchmark problem was proposed, solved and compared against a reference solution computed with PLAXIS 2D V20 (2020). Figure 3a shows a sketch of the benchmark. A square domain, with an elastic drained base, is composed of a homogeneous material characterized by the saturated unit weight γ_{sat}, which is estimated from e_μ and the specific gravity $G_S = 2.65$. Since liquefaction is triggered near point A (see Fig. 3a), this is the position where the computed results are compared against the reference solution. The cyclic behaviour of the soil is modelled with the hypoplastic constitutive model with intergranular strain (Niemunis and Herle 1997; Gudehus et al. 2008) and using the parameters in Table 1. In this benchmark, a mean void ratio $e_\mu = 0.75$ is used. It is observed in Fig. 3b that liquefaction is reached after 4 s, when the effective stresses have dropped to nearly zero and the excess pore water pressure (U) is a maximum. Additionally, it is observed that the results are close to the reference solution, thereby validating the code for simulating liquefaction.

Table 1. Soil parameters

ϕ_c	p_t	h_s	n	e_{d0}	e_{c0}	e_{i0}	α	β	m_R	m_T	R	β_r	χ
(°)	(kPa)	(kPa)	–	–	–	–	–	–	–	–	–	–	–
32	$1.0E^{-5}$	$1.5E^{-6}$	0.27	0.4	0.8	1.1	0.18	1.1	5.0	2.0	$1.0E^{-4}$	0.5	6

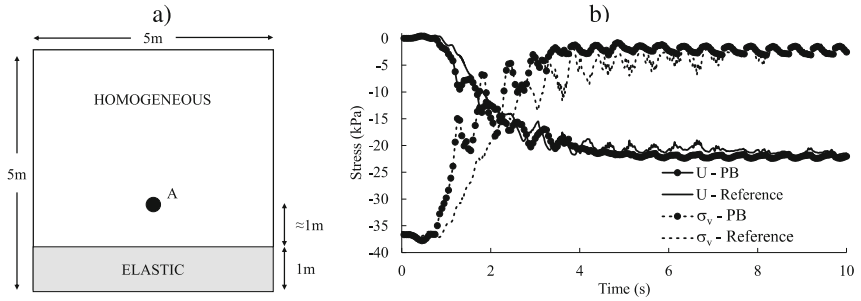

Fig. 3. a) Sketch of the benchmark used for validation purposes, and b) excess pore pressure (U) and vertical effective stress σ_v at point A

4 Results

Liquefaction can be assessed using different indexes. In this paper, two are used and investigated. The first index q_1 considers the ratio between the degradation of the vertical effective stress component (σ_v) and its initial value ($\sigma_{v,i}$). The second index q_2 considers the ratio between U and $\sigma_{v,i}$. Liquefaction is considered to occur when q_1 or $q_2 > 0.95$ using the following equations:

$$q_1 = 1 - \frac{\sigma_v}{\sigma_{v,i}} \tag{1}$$

$$q_2 = \frac{U}{\sigma_{v,i}} \tag{2}$$

The domain used to assess liquefaction considering soil spatial variability is similar to that shown in Fig. 3a, but with a height and width of $h = w = 10$ m and without the elastic base. First, a series of realizations are performed using small scales of fluctuation ($\theta_H = \theta_V = 0.1$ m) and different standard deviations ($e_\sigma = 0.01, 0.1$). Then, additional simulations are performed using the same values of e_σ and increasing the scales of fluctuation to $\theta_H = \theta_V = 2.0$ m. Note that e is the only variable randomized, since it describes the behaviour of the material (i.e. compression or dilation) under shear loading. To compute the most probable liquefaction depth, the indexes q_1 and q_2 are added up for a particular depth of each realization (only if q_1 or $q_2 > 0.95$) and then weighted by the total number of points. Equation (3) illustrates the computation of q_1 for a particular set of realizations and stochastic variables (i.e. e_σ, e_μ, θ_H and θ_V).

$$q_{1,\mu} = \frac{\sum_{r=1}^{nr} \sum_{g=1}^{ngd} 1 - \frac{\sigma_{v,g}}{\sigma_{v,i,g}} > 0.95}{nr \times ngd} \tag{3}$$

where r is the realization number, $\sigma_{v,g}$ and $\sigma_{v,i,g}$ are the current vertical effective stress and initial vertical effective stress at the Gauss point, ngd is the number of Gauss points at a particular depth, and nr is the number of realizations (equal to 50 in this study).

Figure 4 shows the results of the multiple realizations for q_1 as a function of depth. Note that the first meter was ignored, since liquefaction values in that zone can be

unreliable due to the low vertical and horizontal stresses. The properties of the material are the same as shown in Table 1 and the deterministic (D) solution is computed using a constant void ratio of $e_0 = 0.75$. It is observed that the deterministic liquefaction occurs close to a depth of ≈ -5 m, where q_1 is a maximum. Figure 4a and 4b show that, when the standard deviation is small, the average of the stochastic (S) solutions with random fields exhibits a similar liquefaction depth compared to the deterministic solution, regardless of the scales of fluctuation used. In contrast, Fig. 4c and 4d show that, for large e_σ, the similarity with the deterministic solution disappears. Furthermore, the thickness of the liquefaction zone enlarges and moves upwards, reaching the surface in the most extreme condition (i.e. Fig. 4d using $e_\sigma = 0.1$ and $\theta_{H,V} = 2.0$ m).

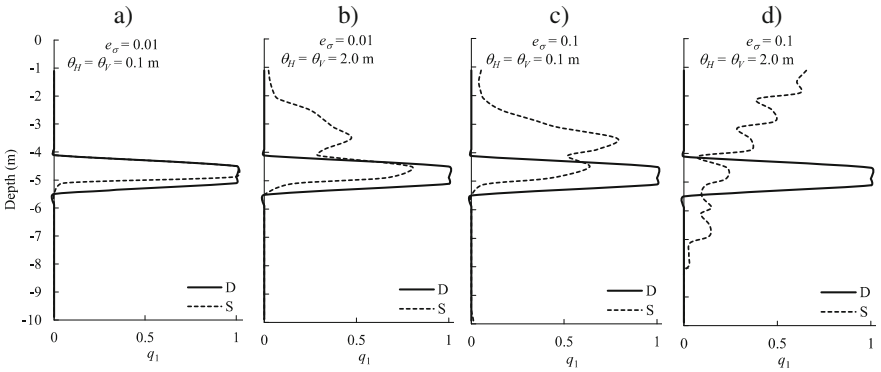

Fig. 4. Computation of q_1 for homogeneous material (i.e. deterministic solution D) and average of stochastic solutions with random fields S, using a) $e_\sigma = 0.01$; $\theta_{H,V} = 0.1$ m, b) $e_\sigma = 0.01$; $\theta_{H,V} = 2.0$ m, c) $e_\sigma = 0.1$; $\theta_{H,V} = 0.1$ m, and d) $e_\sigma = 0.1$; $\theta_{H,V} = 2.0$ m

Figure 5 shows a series of realizations to demonstrate the effect of e_σ on the occurrence of liquefaction in individual realizations. Using $e_\sigma = 0.01$ (Fig. 5a, b, c) the liquefaction depth remains constant and close to -5 m. However, using $e_\sigma = 0.1$ (Fig. 5d, e, f) it is observed that liquefaction can be triggered at different and multiple distinct locations within the same domain. Note that the realizations shown in Fig. 5 consider $\theta_{H,V} = 2.0$ m.

Figure 6 shows results similar to Fig. 4 when using q_2. However, the locations of the peak values are not the same as those when using q_1, indicating that the largest values of U are not necessarily located at depths where the soil has reduced its strength to nearly zero. Additionally, the plots in Figs. 4 and 6 show stochastic values of q_1 and q_2 that do not reach one (i.e. q_1 and $q_2 < 1$), in contrast to the deterministic solution. Considering that the soil always reaches liquefaction at different points (e.g. Fig. 5f), the values in Figs. 4 and 6 indicate the most probable liquefaction depth.

Finally, Fig. 7 shows plots comparing the deterministic (D) surface acceleration against the mean stochastic (S) surface acceleration for single (typical) realizations. Note that the surface acceleration is the mean value of all nodes at the soil surface. It is observed in Fig. 7a that using $e_\sigma = 0.01$ and $\theta_{H,V} = 0.1$ m (i.e. small standard deviation and scale of fluctuation values) the surface acceleration of the stochastic solution is

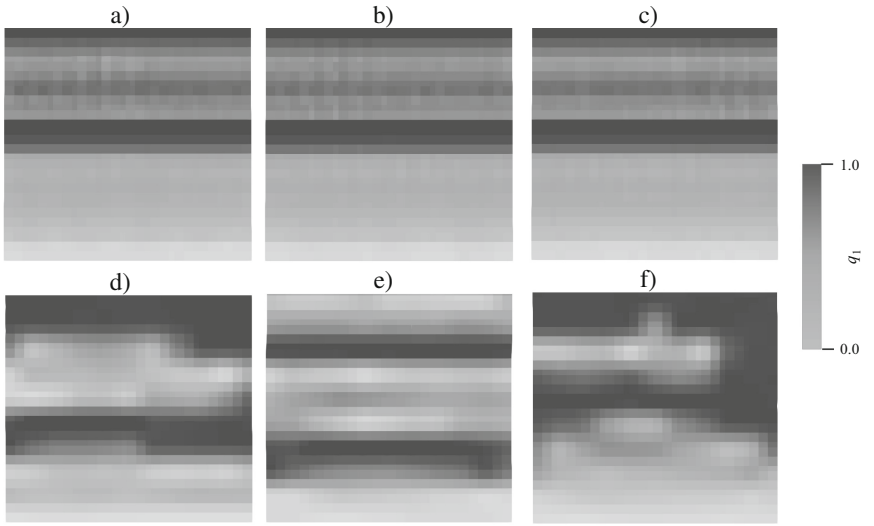

Fig. 5. Liquefaction triggering using $e_\sigma = 0.01$ in realization a) 1, b) 25, and c) 50, and using $e_\sigma = 0.1$ in realization d) 1, e) 25, and f) 50 using scales of fluctuation $\theta_{H,V} = 2.0$ m

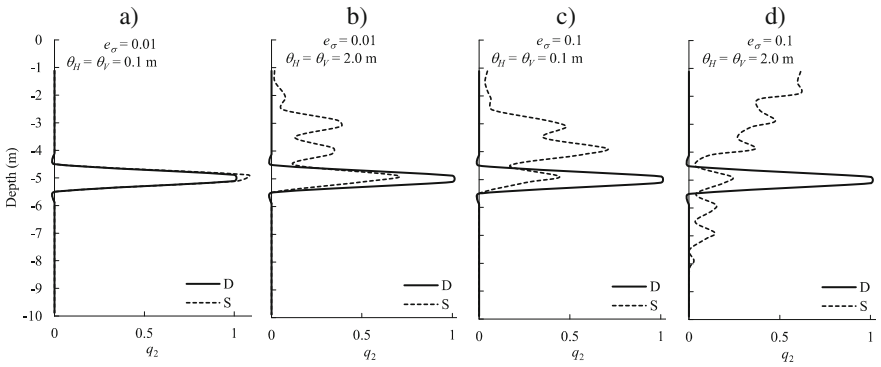

Fig. 6. Computation of q_2 using homogeneous material (i.e. deterministic solution D) and average of stochastic solutions with random fields S, using a) $e_\sigma = 0.01$; $\theta_{H,V} = 0.1$ m, b) $e_\sigma = 0.01$; $\theta_{H,V} = 2.0$ m, c) $e_\sigma = 0.1$; $\theta_{H,V} = 0.1$ m, and d) $e_\sigma = 0.1$; $\theta_{H,V} = 2.0$ m

virtually the same as the deterministic solution, where liquefaction is triggered after 8 s. Figure 7b and 7c show that, by increasing the standard deviation or the scale of fluctuation values (i.e. $e_\sigma = 0.01$ and $\theta_{H,V} = 2.0$ m or $e_\sigma = 0.10$ and $\theta_{H,V} = 0.1$ m), liquefaction occurs earlier, at around 7 s. On the other hand, by using $e_\sigma = 0.1$ and $\theta_{H,V} = 2.0$ m (Fig. 7d), the computed accelerations are very different at around 6 s, with liquefaction being indicated at around 6.5 s. Hence, the results of the example realizations in Fig. 7 suggest that, by increasing the standard deviation and/or scale of fluctuation values, liquefaction may be triggered earlier. Note that the liquefaction triggering time is estimated base on the drop of acceleration observed in Fig. 7.

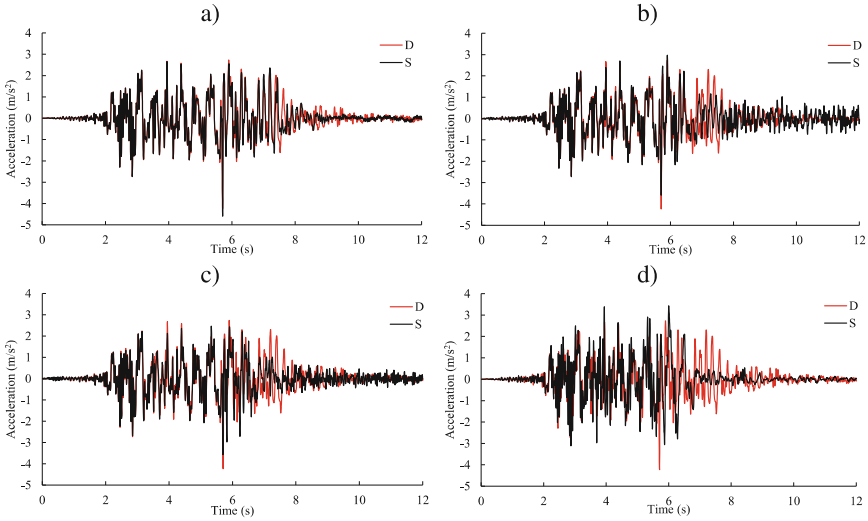

Fig. 7. Comparison of deterministic D surface acceleration and mean stochastic S surface acceleration for specific realizations, using a) $e_\sigma = 0.01$; $\theta_{H,V} = 0.1$ m, b) $e_\sigma = 0.01$; $\theta_{H,V} = 2.0$ m, c) $e_\sigma = 0.1$; $\theta_{H,V} = 0.1$ m, and d) $e_\sigma = 0.1$; $\theta_{H,V} = 2.0$ m

5 Conclusions

Liquefaction has been assessed using stochastic soil properties and two different indexes, q_1 and q_2. It has been shown that the standard deviation values have a more significant impact on the results compared to the scale of fluctuation values (for the range of values considered). Small values of e_σ show a tendency for the results to approximate the deterministic solution. However, large values of e_σ can return results far from the deterministic solution, although, if the scales of fluctuation are small, then the effects of using a large standard deviation can diminish due to the averaging of material properties. It was observed that, by using large standard deviation and scale of fluctuation values, the liquefaction zone thickness grew and moved upwards to shallower positions. Regarding the use of q_1 and q_2, both indexes show similar results. Nevertheless, since the q_2 results are not the same as those for q_1, it can be concluded that the decrease in vertical effective stress is not necessarily accompanied by an equal increment of pore pressure, mainly due to the spatial distribution of soil properties.

Acknowledgements. This work is part of the research programme DeepNL/SOFTTOP with project number DEEP.NL.2018.006, financed by the Netherlands Organisation for Scientific Research (NWO).

References

Cook, R.D., Malkus, D.S., Plesha, M.E.: Concepts and Applications of Finite Element Analysis, 3rd edn. Wiley, New York (1989)

Fenton, G.A., VanMarcke, E.H.: Spatial variation in liquefaction risk. Géotechnique **48**(6), 819–831 (1998)

Gudehus, G., et al.: The soilmodels.info project. Int. J. Numer. Anal. Methods Geomech. **32**(12), 1571–1572 (2008)

Hicks, M.A., Samy, K.: Influence of heterogeneity on undrained clay slope stability. Q. J. Eng. Geol. Hydrogeol. **35**(1), 41–49 (2002)

Niemunis, A., Herle, I.: Hypoplastic model for cohesionless soils with elastic strain range. Mech. Cohesive-Frictional Mater. **2**(4), 279–299 (1997)

PLAXIS 2D, V20: Bentley Systems, Incorporated, Dublin (2020)

Popescu, R., Prevost, J.H., Deodatis, G.: 3D effects in seismic liquefaction of stochastically variable soil deposits. Géotechnique **55**(1), 21–31 (2005)